Smooth Phases, Roughening Transitions and Novel Exponents in One-dimensional Growth Models.

U. Alon[1,2], M. R. Evans[3], H. Hinrichsen[4], and D. Mukamel[1]

[1] *Department of Physics of Complex Systems, Weizmann Institute, Rehovot 76100, Israel*
[2] *Present address: Depts. of Molecular Biology and Physics, Princeton University, Princeton NJ 08540*
[3] *Department of Physics and Astronomy, University of Edinburgh, Mayfield Road, Edinburgh EH9 3JZ, U.K.*
[4] *Max-Planck-Institut für Physik komplexer Systeme, Nöthnitzer Straße 38, D-01187 Dresden, Germany*

(October 14, 1997, submitted to Phys. Rev. E)

A class of solid-on-solid growth models with short range interactions and sequential updates is studied. The models exhibit both smooth and rough phases in dimension $d = 1$. Some of the features of the roughening transition which takes place in these models are related to contact processes or directed percolation type problems. The models are analyzed using a mean field approximation, scaling arguments and numerical simulations. In the smooth phase the symmetry of the underlying dynamics is spontaneously broken. A family of order parameters which are not conserved by the dynamics is defined as well as conjugate fields which couple to these order parameters. The corresponding critical behavior is studied and novel exponents identified and measured. We also show how continuous symmetries can be broken in one dimension. A field theory appropriate for studying the roughening transition is introduced and discussed.

PACS numbers: 05.40.+j; 05.70.Ln; 68.35.Fx; 64.60.Ak

I. INTRODUCTION

The statistical properties of moving interfaces and surfaces of growing crystals have been studied extensively in recent years [1]. Various theoretical approaches have been applied in these studies including field theoretical analyses of continuum KPZ-type equations [2–4] and studies of discrete growth processes such as solid-on-solid (SOS) or polynuclear growth (PNG) models amongst others [4–14].

One of the more interesting properties of moving interfaces is their roughness. It is well known that in $d > 2$ dimensions, moving interfaces may be either rough or smooth depending on the level of the noise in the system. However, growth processes in $d = 1$ dimensions are more subtle. Most growth processes governed by short range interactions, such as those described by the KPZ equation yield a rough interface. On the other hand study of a class of PNG models suggested that both smooth and rough phases may exist in one dimension ($1d$) [9,15,16]. However, this class of models is characterized by two key features: (a) The evolution takes place by a parallel updating process in which time progresses in discrete steps and all sites of the interface are updated simultaneously according to a given rule at any given time step. Such dynamics tend to be less noisy than sequential updating processes, in which one site is updated at a time. (b) The models have a maximal velocity by which the uppermost point of the surface can propagate. The existence of a maximal velocity in these models is due to the use of parallel updates, and the smooth phase disappears when random sequential (continuous time) updates are used. An interesting question is whether a sequential update growth process is capable of exhibiting smooth and rough phases in $1d$.

Some time ago a transition from a smooth to a rough surface was observed in a SOS model for surface reconstruction with sequential updates and particle conservation [11]. The free parameter, H, is the maximal allowed height difference between adjacent sites and is a discrete quantity. It was observed that the surface is smooth for $H < 3$ and macroscopically grooved for $H > 3$. At $H = 3$ the surface appears to be rough. This phenomenon is clearly related to the local conservation law in this model.

Recently, a class of growth processes with short range interactions, sequential updates and non-conserved dynamics was introduced [17]. They were demonstrated to exhibit both rough and smooth phases in $1d$. The dynamics is described by SOS models in which adsorption and desorption processes take place in a ring geometry. Depending on the relative rates of the two processes one finds either a smooth or a rough phase. In studying the roughening transition in these models, it has been found that some of its features are related to those of contact processes, or directed percolation, which have been extensively studied in the past [18–21]. These latter systems exhibit a continuous phase transition which is strongly linked to the existence of absorbing states (a set of states from which the system can not escape). The model introduced in [17] may be viewed as composed of a series of contact processes interacting with each other, whose dynamics does not have an absorbing state. This model is the subject of the present paper.

An intriguing question related to the existence of a smooth phase is that of spontaneous symmetry breaking (SSB) and long-range order in 1d systems with short-range interactions and small but unbounded noise. By unbounded noise we mean that in a finite system all microscopic configurations can be reached from any initial condition in a finite time. It is well known that in ther-

mal equilibrium no phase transition takes place under these conditions. Systems far from equilibrium [22] such as moving interfaces or driven diffusive systems are, however, less restrictive and the question of existence of SSB under these conditions has been open for some time. Recently, a simple non-equilibrium model which exhibits SSB in $1d$ was introduced [23,24]. This model belongs to a class of driven-diffusive systems, in which charges of two kinds are injected at the ends of a 1d lattice and are biased to move in opposite directions. The dynamic rules are symmetric under space and charge inversion (PC invariance). However, this symmetry is broken in the stationary state of the system where the currents of the two charge species are different. In this model, SSB is the result of the *conserved* order parameter in the bulk (charges are not created or annihilated except at the boundaries), and the existence of *open* boundary conditions. These two conditions favor the emergence of SSB; the conserved dynamics slows down the temporal evolution of the system, moreover flips from one broken symmetry phase to another can originate only at the boundaries where the order parameter is not conserved. Initial attempts to modify this model such that either or both of these features are eliminated resulted in symmetric stationary states with no SSB.

The growth model discussed in the present work provides a simple example for SSB which takes place far from equilibrium. The breaking of symmetry takes place in the smooth phase and the order parameter associated with this transition is not conserved by the dynamics. The model thus demonstrates that SSB can take place in $1d$ in non-equilibrium systems with non-conserved order parameter and ring geometry.

In this paper we present a detailed analysis of the growth models introduced in [17]. The relation of the models to contact processes and directed percolation is discussed and several families of novel critical exponents are defined. One family describes the critical behavior of magnetization-like order parameters related to the symmetry breaking. Another family is related to statistical properties of the interface height near the roughening transition. The dynamical equations are analyzed using the mean field approximation, and a field theoretical model appropriate for the roughening transition is introduced. The scaling picture that emerges is far from complete but points to the existence of complex critical behavior.

The paper is organized as follows: The growth model is defined in Sec. II. The relation to contact processes and directed percolation is discussed in Sec. III. In Sec. IV the results of scaling analysis and numerical studies are presented. The question of spontaneous symmetry breaking, and the family of order parameters and their critical behavior are discussed in Sec. V. The dynamics of the model is studied within the mean field approximation in Sec. VI, and a field theoretical model appropriate for studying the critical behavior of the roughening transition is defined and discussed in Sec. VII. In Sec. VIII some light is shed on the relation of the model to the polynuclear growth models discussed above and in Sec. IX the main results are summarized and conclusions drawn. Finally, a particular case for which steady state can be calculated exactly is presented in Appendix A.

II. MODEL DEFINITIONS

The class of models is most simply introduced in terms of the growth of a one dimensional interface, in which both adsorption and desorption processes take place. In the present models the key feature is that desorption may take place only at the edge of a plateau, i.e. at a site which has at least one neighbor at a lower height. We study two particular models in this class, (a) a restricted solid on solid (RSOS) version where the height differences between neighboring sites are restricted to take values $1, 0, -1$ and (b) an unrestricted model where there is no such restriction. Both models are defined on a 1d lattice of N sites $i = 1 \dots N$ and associated with each site is an integer height variable h_i which may take values $0, 1 \dots \infty$. Periodic boundary conditions are imposed so that $h_{N+i} = h_i$.

The dynamics are defined through the following algorithm: at each update choose a site i at random and carry out one of the following processes: Adsorption of an adatom

$$h_i \to h_i + 1 \ \text{ with probability } q \tag{1}$$

or desorption of an adatom from the edge of a step

$$h_i \to \min(h_i, h_{i+1}) \ \text{ with probability } (1-q)/2 \tag{2}$$
$$h_i \to \min(h_i, h_{i-1}) \ \text{ with probability } (1-q)/2 \tag{3}$$

The update of the chosen site i is conveniently implemented in a simulation by drawing a random number between 0 and 1 from a flat distribution. If the number is less than q process (1) is executed, if the number is greater than $(1+q)/2$ process (2) is executed, otherwise process (3) is executed.

In the RSOS version, a process is only carried out if it respects the constraint

$$|h_i - h_{i+1}| \leq 1 \ . \tag{4}$$

For both models, when the growth rate q is low, the desorption processes (2)–(3) dominate. If all the heights are initially set to the same value this layer will remain the bottom layer of the interface. Small islands will grow on top of the bottom layer through the process (1) but will quickly be eliminated by desorption at the island edges. Thus, the interface is effectively anchored to its bottom layer and the velocity, defined as the rate of increase of the minimum height of the interface, is zero in the thermodynamic limit. On a finite system, very large fluctuations will occasionally occur which allow a new

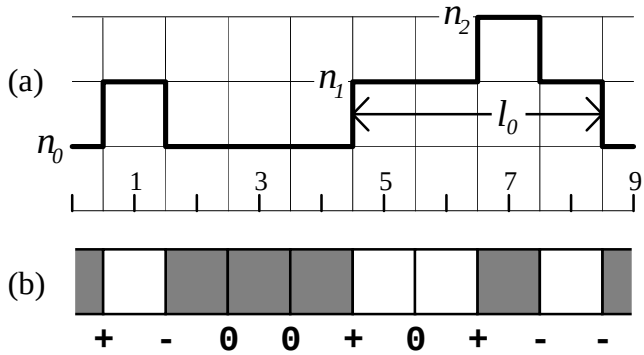

FIG. 1. (a) Typical configuration of the interface. n_k is the fraction of sites at height k above the minimal height in the configuration (here $n_0 = n_1 = \frac{4}{9}$, $n_2 = \frac{1}{9}$). The average island size grown on top of level k is l_k. (b) Mapping of the configuration of Fig.1a to the charged-particle representation (see Eq. 11), along with a site coloring, as described in Sec. V.

layer to be completed and the velocity will be positive but exponentially small in the system size.

As q is increased the production of islands on top of the bottom layer increases until above q_c, the critical value of q, the islands merge and new layers are formed at a finite rate giving rise to a finite interface velocity in the thermodynamic limit. Thus, above the transition one expects the velocity to behave as

$$v \sim (q - q_c)^y \,, \tag{5}$$

where y is the critical exponent describing the growth in velocity.

Another critical exponent is defined by considering n_0, the fraction of sites at the lowest level (see Fig. 1). Below the transition ($q < q_c$) this fraction will be large since the interface is anchored at this level. As the transition is approached more and more islands form on top of the bottom layer and the fraction n_0 will decrease until it vanishes at the transition. This may be described by

$$n_0 \sim (q_c - q)^{x_0} \,. \tag{6}$$

Similarly one may define a family of exponents $\{x_k\}$ describing the vanishing of n_k, the fraction of sites at level k,

$$n_k \sim (q_c - q)^{x_k} \,. \tag{7}$$

The interface width is defined by

$$W = [N^{-1} \sum_i (h_i - N^{-1} \sum_j h_j)^2]^{1/2} \,. \tag{8}$$

Below the transition the width should be finite indicating a smooth interface exploring only a finite height above the bottom layer. However, above the transition the interface should display the behavior generic to moving interfaces [2], that is roughening where the width diverges as

$$W \sim N^{1/2} \qquad \text{at } q > q_c \,. \tag{9}$$

Therefore near to and above the transition we expect

$$W \sim N^{1/2} (q - q_c)^{\chi} \,, \tag{10}$$

where χ is the exponent describing the vanishing of the roughness as the transition is approached.

The above considerations hold for both RSOS and unrestricted models and and we will address the question as to what extent the two models can be seen as representatives of a whole class of models with the same critical behavior. In Sec. IV we will further explore the scaling behavior, adding to the exponents y, x_k, χ that we have so far introduced. However, we defer this until after Sec. III where we discus the relation to a directed percolation model through which some of the simple critical behavior may be understood.

For the moment we note that the RSOS version (4) may be viewed as a driven diffusion model of two oppositely charged types of particles. The charges

$$c_i \;=\; h_i - h_{i-1} \;\in\; \{-\,,\; 0\,,\; +\} \tag{11}$$

are bond variables and represent a change of height between adjacent interface sites (see Fig. 1). In this representation, it is convenient to convert the dynamical rules (1)-(3) into processes occurring at bonds with the following *rates*

$$\begin{aligned}
0\,+ \;&\rightarrow\; +\,0 \quad \text{with rate } g \\
+\,0 \;&\rightarrow\; 0\,+ \quad \text{with rate } 1 \\
-\,0 \;&\rightarrow\; 0\,- \quad \text{with rate } g \\
0\,- \;&\rightarrow\; -\,0 \quad \text{with rate } 1 \\
0\;\,0 \;&\rightarrow\; +\,- \quad \text{with rate } g \\
+\,- \;&\rightarrow\; 0\;\,0 \quad \text{with rate } 2 \\
-\,+ \;&\rightarrow\; 0\;\,0 \quad \text{with rate } g
\end{aligned} \tag{12}$$

where the growth rate g is related to q of equations (1)–(3) through

$$g = 2q/(1-q) \,. \tag{13}$$

The rule that desorption cannot occur from the middle of a plateau corresponds to the absence of the process $0\,0 \rightarrow -\,+$. In this version the dynamics may be performed without reference to the height variables h_i (although these can easily be reconstructed to within the height of the bottom layer from the variables c_i). The critical behavior is reflected in the correlations between the charges. At $q < q_c$, the charges are arranged as closely bound $+\,-$ dipoles. At $q > q_c$, the dipoles become unbound, and the fluctuations in the total charge, measured over a distance of order N, diverge with N.

The charged particle representation also allows the effect of desorption from the middle of a plateau to be studied. This is done in Appendix A by introducing a non-zero rate p for the process $0\,0 \rightarrow -\,+$ and solving

the steady state exactly in the case $p = 1 - g/2$. The result is that, although different choices of this rate allow the interface velocity to be positive, zero or negative, the interface is always rough and no smooth phase exists.

III. RELATION TO DIRECTED PERCOLATION AND CONTACT PROCESSES

Some of the critical behavior described in the previous section may be related to that of directed percolation (DP). In DP sites of a lattice are either occupied by a particle or empty. The dynamical processes are that a particle can self-annihilate or produce an offspring at a neighboring empty site. If the rate of self-annihilation is sufficiently high the system always reaches an absorbing state where no particles remain and therefore no further particle can be produced. On the other hand when the rate of offspring production is high, another steady state of the system, where the density of particles is finite, exists on the infinite lattice and is termed the active phase.

In DP the dynamics is usually carried out in parallel, e.g. [21]. In the corresponding models in the mathematical literature, known as contact processes [19], the dynamics are defined in continuous time which can be numerically implemented by random sequential dynamics.

To see the analogy with the growth model defined in Sec. II consider the dynamics of the bottom layer of the unrestricted model. Let us introduce variables $\{s_i\}$ which take value 1 if the height of site i is that of the bottom layer and take value zero otherwise. The algorithm stated in (1)–(3) is exactly equivalent to the following dynamics for the $\{s_i\}$. At each update randomly select a site i and modify s_i with the following probabilities

$$\begin{aligned}
&\text{if } s_i = 1 \\
&\qquad s_i \to 0 \text{ with prob. } q \\
&\text{if } \{s_{i-1}, s_i, s_{i+1}\} = \{0,0,1\} \\
&\qquad s_i \to 1 \text{ with prob. } (1-q)/2 \\
&\text{if } \{s_{i-1}, s_i, s_{i+1}\} = \{1,0,0\} \\
&\qquad s_i \to 1 \text{ with prob. } (1-q)/2 \\
&\text{if } \{s_{i-1}, s_i, s_{i+1}\} = \{1,0,1\} \\
&\qquad s_i \to 1 \text{ with prob. } 1-q
\end{aligned} \tag{14}$$

This dynamics is exactly that of a contact process when we take $s_i = 1$ to indicate the occupation of a site: the particles self-annihilate with rate $\lambda = q/(1-q)$ and a particle is created at a vacant site with rate $1/2$ if one neighbor is occupied and rate 1 if both neighbors are occupied. This process has been extensively studied by series expansions [25] and short time expansions [26] and the transition found to occur at $\lambda_c \simeq 0.3032$ corresponding to $q_c \simeq 0.2327$ for the unrestricted growth model. Thus, as seen by the bottom layer of the growing interface, the transition from anchored to moving phase is simply a DP transition. The anchored phase corresponds to the active DP phase whereas the moving phase corresponds to the absorbing DP phase.

The critical behavior of DP may be described as follows. Above the transition ($\lambda > \lambda_c$) an initial seed particle will typically produce activity over a region of lateral extent $\xi_\perp \sim |\epsilon|^{-\nu_\perp}$ and duration $\xi_\parallel \sim |\epsilon|^{-\nu_\parallel}$, before the absorbing state is reached. Here ϵ, given by

$$\epsilon = q - q_c \,, \tag{15}$$

measures how far the system is from criticality and $\xi_\perp$ and $\xi_\parallel$ are interpreted as spatial and temporal scaling lengths which diverge at the transition. Below the transition ($\lambda < \lambda_c$) the density n of occupied sites in the active phase is $n \sim |\epsilon|^\beta$ and there is a finite probability $|\epsilon|^\beta$ that an initial seed particle will result in the active phase being reached. The lateral extent of such an active cluster grows with time as t^z where $z = \nu_\parallel/\nu_\perp$ is the dynamic exponent. The typical size l of regions containing no activity diverges as the transition is approached as $l \sim n^{-1} \sim |\epsilon|^{-\beta}$.

These exponents allow one to readily identify y and x_0 defined in Eqs. (5) and (6). Since n_0 corresponds to the density of occupied sites in the DP active phase we expect in (6)

$$n_0 \sim (q_c - q)^\beta \;\text{ and }\; x_0 = \beta \,. \tag{16}$$

In the moving phase the velocity is given by the inverse of the typical time for the bottom layer to be covered over. We identify this time scale with the lifetime of active regions in the DP absorbing phase and we expect in (5)

$$v \sim 1/\xi_\parallel \sim (q - q_c)^{\nu_\parallel} \;\text{ and }\; y = \nu_\parallel \,. \tag{17}$$

Thus we see that the two exponents x_0 and y that describe quantities involving *only* the dynamics of the bottom layer may be directly identified with known (numerically) DP exponents. Exponents describing quantities involving higher levels of the growth process such as x_k given by (7) are not so straightforward as we shall see in Secs. IV and V.

In this section the exact mapping of the bottom layer of the unrestricted growth model to DP has been described. For the RSOS model there is no such exact mapping, nevertheless we expect the bottom layer to exhibit DP behavior and relations (16),(17) to hold, because the phase transition in this model should display a robustness with respect to the microscopic rules similar to that found in DP models.

IV. SCALING AND NUMERICAL RESULTS

So far we have seen that as criticality is approached from the smooth phase the scaling properties of some quantities involving only the bottom level of the interface may be adequately described using DP exponents.

However, for more general quantities the scaling is less clear cut and indeed only a partial picture emerges. We first deal with properties of the first few layers in the smooth phase using heuristic arguments and then comparing them to numerical results. The width W, a quantity involving all layers, is studied next. It is argued that a simple scaling picture, involving only the DP correlation length $\xi_\perp$, does not hold. We provide evidence to suggest that other length scales may be important as criticality is approached from within the moving phase. A partial scaling picture which emerges is then summarized.

A. Scaling properties of the first few layers

We now discuss the scaling properties of the first few layers $k = 1, 2, \ldots$ above the bottom layer. Since, in the smooth phase, the scaling properties at the bottom layer ($k = 0$) are completely characterized by the three DP exponents $x_0 = \beta$, $\nu_\perp$, and $\nu_{||}$, it is natural to assume that the next layers obey similar scaling laws with analogous exponents, $x_k = \beta^{(k)}$, $\nu_\perp^{(k)}$, and $\nu_{||}^{(k)}$, where, for example, x_k is the density exponent defined in Eq. (7). In principle all these exponents could be different and independent. Our numerical results, however, suggest that the scaling exponents $\nu_\perp^{(k)}$ and $\nu_{||}^{(k)}$ are *identical on all levels* and equal to the DP exponents $\nu_\perp$ and $\nu_{||}$. This remarkable property implies that the growth process at criticality is characterized by a *single* anisotropy exponent $z = \nu_{||}/\nu_\perp$. On the other hand we find numerically that the density exponents x_k for $k = 1, 2, \ldots$ are different and considerably reduced compared to their DP value $x_0 = \beta$. It appears that these exponents are non-trivial in the sense that they are not simply related to DP exponents.

In order to explain the reduced values of x_k, we present a simple heuristic argument [17]. Let us first consider the bottom layer $k = 0$. As explained in the previous section, DP is characterized by two length scales: the average size of inactive islands $l_0 \sim n_0^{-1} \sim |\epsilon|^{-\beta}$, and the spatial scaling length $\xi_\perp \sim |\epsilon|^{-\nu_\perp}$ [27]. They both are related, for a system of size N, by the finite size scaling relation $l_0 \sim |\epsilon|^{-\beta} f(N|\epsilon|^{\nu_\perp})$, where f is a function satisfying $f(s) \sim s^{\beta/\nu_\perp}$ for $s \to 0$, implying that on a finite system at criticality one has $n_0 \sim l_0^{-1} \sim N^{-\beta/\nu_\perp}$. Now consider the next layer $k = 1$. One may view the sites at heights $k \geq 2$ as islands of active sites growing on top of the inactive islands of the $k = 1$ level, whose typical size is l_0. Applying the same scaling relations and assuming that the system size may be replaced by l_0, we find $n_1 \sim l_1^{-1} \sim l_0^{-\beta/\nu_\perp}$, where l_1 is the mean size of islands of sites with height $k \geq 2$. Repeating this argument one obtains $n_k \sim l_k^{-1} \sim l_{k-1}^{-\beta/\nu_\perp}$ and therefore

$$n_k \sim |\epsilon|^{x_k}, \quad x_k = \beta(\beta/\nu_\perp)^k . \tag{18}$$

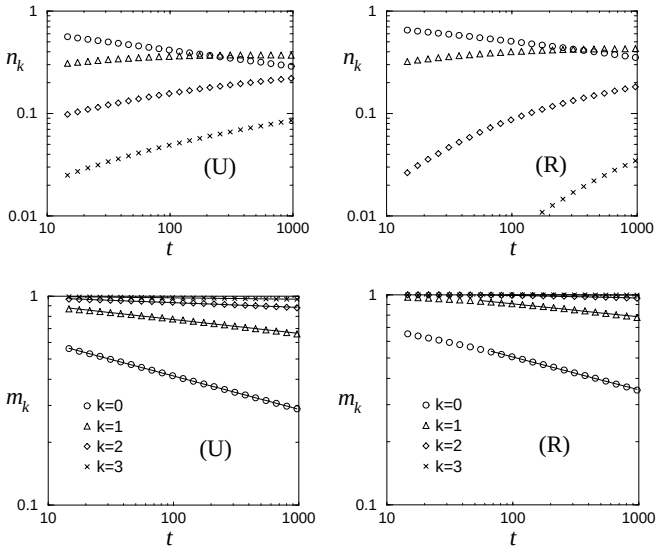

FIG. 2. Dynamic simulations: the densities n_k and the integrated densities m_k at criticality as a function of time t in the (U) unrestricted and (R) restricted growth model. See Eq. (19).

Inserting the numerically known DP exponents [28]

$$\beta = 0.27649(4), \quad \nu_{||} = 1.73383(2), \quad \nu_\perp = 1.09684(2)$$

we obtain the approximations $x_1 \simeq 0.070$, $x_2 \simeq 0.017$, and $x_3 \simeq 0.004$ which are in qualitative agreement with the numerical results (see below). However, this simple scaling argument is not quantitatively correct for several reasons. First we consider the temporal average of the island size l_0 as a fixed 'finite size' length for a DP process taking place on top of the island; we thus neglect the temporal fluctuations of l_0. In addition, unlike exact scaling relations, our scaling argument is expected to fail in higher dimensions since it is derived in the case of one dimension where active sites separate inactive island. Nevertheless it can be used as a rough approximation as well as qualitative explanation for the strongly reduced values of x_k compared to x_0 for $k \geq 1$.

B. The first few layers - numerical results

In order to determine the density exponents x_k and to verify that the scaling exponents $\nu_\perp^{(k)}$ and $\nu_{||}^{(k)}$ are indeed identical, we employ three different variants of Monte-Carlo (MC) simulations, termed dynamic, static and finite size simulations, described as follows.

Dynamic simulations: First we measure the temporal evolution of the densities n_k at criticality in a large system, starting from a flat interface and averaging over a large number of runs. For times larger than some transient time the densities are expected to decay according to

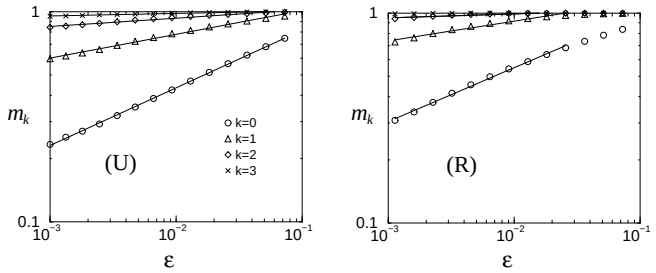

FIG. 3. Static simulations: double logarithmic plot of the saturation value of the integrated densities m_k vs $|\epsilon|$. See Eq. (20).

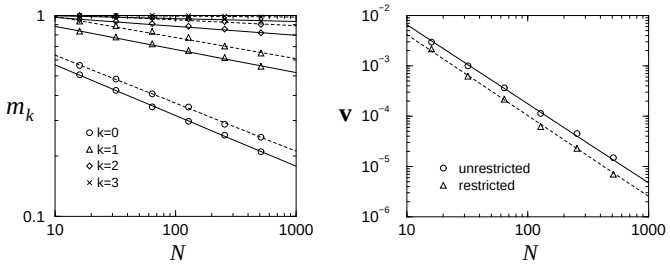

FIG. 4. Finite size simulations: Measurement of the integrated densities m_k and the growth velocity v at criticality as function of the system size N. The solid (dashed) lines refer to the unrestricted (restricted) model. See Eq. (21).

$$n_k \sim t^{-x_k/\nu_{||}} \,. \tag{19}$$

Static simulations: We also determine x_k directly in off-critical (static) simulations, measuring the densities n_k in a sufficiently large system in the smooth phase and averaging over very long times. Using this method we can determine the exponents x_k directly through the expected behavior

$$n_k \sim |\epsilon|^{x_k} \,, \tag{20}$$

where $\epsilon = q - q_c < 0$.

Finite size simulations: Finally we analyze the finite size scaling of n_k in critical systems of size N averaged over long times. Here the expected scaling behavior reads

$$n_k \sim N^{-x_k/\nu_\perp} \,. \tag{21}$$

Thus the dynamic simulation should yield a numerical value for $x_k/\nu_{||}$, the static simulation a value for x_k and the finite size simulation a value for $x_k/\nu_\perp$. If, on inserting the DP values of $\nu_{||}$ and $\nu_\perp$, the three methods (19)-(21) lead to the same numerical result for the exponent x_k, to within numerical errors, we may conclude that the scaling exponents $\nu_\perp^{(k)}$ and $\nu_{||}^{(k)}$ are indeed equal to the DP exponents.

We observed that the quality of the numerical results can be improved considerably if we measure the *integrated densities*

		dynamic method	static method	finite size method
x_0	U:	0.275(5)	0.273(10)	0.276(5)
	R:	0.270(10)	0.277(10)	0.265(10)
x_1	U:	0.114(5)	0.110(10)	0.125(5)
	R:	0.108(10)	0.110(10)	0.118(10)
x_2	U:	0.039(15)	0.035(15)	0.045(10)
	R:	0.022(15)	0.025(20)	0.033(15)
x_3	U:	0.011(10)	no result	0.015(10)
	R:	no result	no result	no result

TABLE I. Numerical estimates for the density exponents $x_0, \ldots, x_3$ for (U) the unrestricted and (R) the restricted version of the growth model obtained by various simulation methods.

$$m_k = \sum_{j=0}^{k} n_j \tag{22}$$

instead of the densities n_k. The integrated density m_k is the probability of finding the interface at height $h \leq k$. Since $x_{k-1} > x_k$, we have $n_{k-1} \ll n_k$ near criticality and therefore m_k and n_k scale asymptotically with the same exponents. The difference between the two quantities is illustrated for the case of dynamic simulations at q_c in Fig. 2 (for the method of determining q_c see below). As one can see, the graph for the integrated densities m_k in the unrestricted model shows almost perfect straight lines in a double logarithmic representation while the corresponding curves for n_1, n_2 and n_3 still increase which makes it impossible to determine the corresponding exponents with the 1000 time steps illustrated. The same observation, although with less numerical accuracy, holds for the restricted model. Therefore, instead of n_k, we always measure the integrated densities m_k for which we assume the same scaling as in Eqs. (19)-(21).

The dynamic MC simulations are performed on a large system with $N = 10^4$ sites starting from a flat interface. Detecting deviations from the power law behavior, we find the critical points $q_c = 0.23267(3)$ for the unrestricted and $q_c = 0.1889(1)$ for the restricted model (corresponding to $g = 0.4658$ in Eq. (13)). The time dependence of m_k at criticality is averaged over typically 10^5 independent runs. The results are shown in Fig. 2. From the slopes we estimate the critical exponents $x_k/\nu_{||}$. Using $\nu_\parallel$ of DP we obtain the exponents x_k which are summarized in the left column of Table I.

We note a numerical puzzle we have so far failed to explain. The critical value of q for the restricted model appears to be given to high numerical accuracy by $q_u/(1-q_u)$ where q_u is the critical value of the unrestricted model. Whether this is sheer coincidence or whether it is a manifestation of some duality between the two models is an open question.

Static simulations are then carried out in the smooth phase $q < q_c$. Varying $|\epsilon| = q_c - q$ from 10^{-3} to 10^{-1} we first equilibrate the interface on a large lattice with $N = 10^4$ sites over a time interval up to 10^5 time steps.

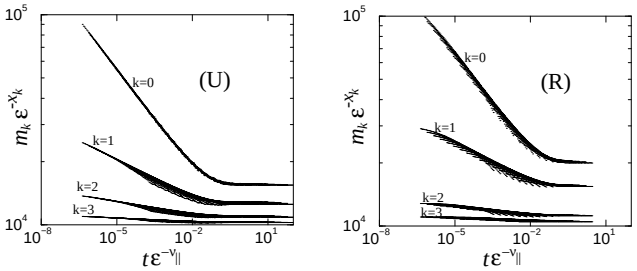

FIG. 5. Finite time static simulations: Data collapse for the scaled integrated densities m_k as a function of time measured in the smooth phase for various values of ϵ in the case of (U) the unrestricted and (R) the restricted growth model.

Then the stationary densities m_k are averaged over a time interval of the same size. The results are again averaged over 100 independent runs. Using this method we can estimate the critical exponents x_k directly from the slopes of the lines in Fig. 3 (see middle column in Table I).

Finally finite-size simulations at criticality are carried out for various lattice sizes $N = 8, 16, 32, \ldots, 1024$. Starting from a flat interface we averaged the integrated densities m_k over time intervals proportional to N^z, ranging from 5000 time steps for $N = 8$ up to $3 \cdot 10^7$ time steps for $N = 1024$. Since finite sized systems at criticality have a small but finite growth rate, the densities m_k have to be measured with respect to the actual lowest level of the interface, i.e. in a co-moving frame. The slopes of the curves in Fig. 4 give an estimate of $x_k/\nu_\perp$ (and therewith x_k, see right column of Table I). In addition, the finite growth rate measured in this type of simulation is expected to scale as $v \sim N^{-y/\nu_\perp}$ which allows an estimate of the exponent y in Eq. (17). Our results are $y = 1.71(5)$ for the unrestricted and $y = 1.76(10)$ for the restricted model (see Fig. 4) which is in agreement with our scaling prediction $y = \nu_\parallel \simeq 1.734$ in Eq. (17).

As a final check of scaling we can also obtain a finite time collapse using the short time data from static simulations. In the smooth phase the expected scaling is $m_k(t) \sim |\epsilon|^{x_k} f_k(t|\epsilon|^{\nu_{||}})$, where $f_k(s) \to const$ for $s \to \infty$ and $f_k(s) \sim s^{-x_k/\nu_{||}}$ for $s \to 0$. Fig. 5 shows the scaling functions $f_k(s)$ for various values of ϵ ranging from -10^{-4} to -0.07 measured up to 10^4 time steps. The long time stationary values of the densities m_k in static simulations (20) correspond to the saturation levels of the different curves.

Since the three different methods lead to the same results for x_k within numerical errors, we conclude that the scaling exponents $\nu_\perp^{(k)}$ and $\nu_{||}^{(k)}$ are indeed identical on all levels and equal to the DP exponents $\nu_\perp$ and $\nu_{||}$. We obtain the DP exponent $x_0 = \beta$, as expected at the bottom layer, while $x_1 \simeq 0.12, x_2 \simeq 0.04, x_3 \simeq 0.015, \ldots$. These latter exponents, although showing the same trend, are clearly different numerically from those obtained using the heuristic picture of subsection IV A. It is not clear whether $\{x_k\}$ for $k > 0$ are related to the DP exponents or whether they are independent exponents. The fact that we obtain the same exponents in the restricted and the unrestricted model suggests that both variants – at least with respect to the first few layers – belong to the same universality class.

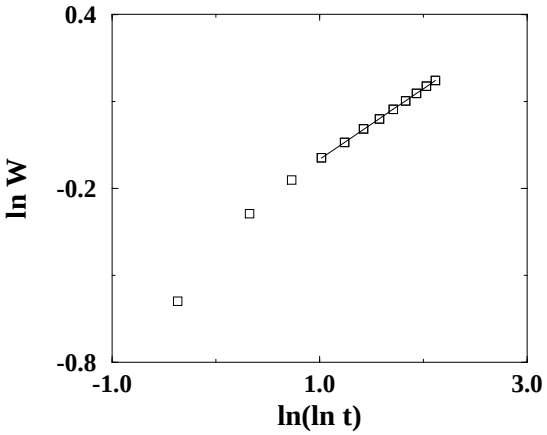

FIG. 6. Width at criticality as a function of time in the unrestricted model. The graph is for $N = 2048$ and shows the growth of the width starting from a flat interface averaged over 2000 runs. The straight line is a best fit through the long time points (2^6—2^{13} MCS) and has a slope of 0.24.

C. Scaling of the Interface Width

In this subsection we investigate the scaling properties of the interface width, defined by (8), at criticality and as the rough phase is entered. The latter measurements lead us to conclude that a complicated scaling behavior prevails.

First recall that in the smooth phase the interface explores only a finite number of levels and the width is finite. In the rough phase the width is expected to diverge according to $W \sim N^{1/2}$, the behavior generic to moving interfaces in one dimension [2].

A naive scaling picture would suggest that the interface width may be written as $W \sim |\epsilon|^{-\eta} f(N/\xi_\perp) \sim |\epsilon|^{-\eta} f(N|\epsilon|^{\nu_\perp})$, where η is some critical exponent. We refer to this picture as naive because implicit is the simple scaling assumption of a single length scale in the problem, a point we shall question in Sec. IV D. Within this naive picture one chooses a scaling function f so as to obtain the expected $\sqrt{N}$ behavior in the rough phase. This leads to the following small ϵ, large N asymptotic limits:

$$\begin{array}{ll} W \sim |\epsilon|^{-\eta} & \text{for } \epsilon < 0 \\ W \sim N^{\eta/\nu_\perp} & \text{for } \epsilon = 0 \\ W \sim N^{1/2}\,\epsilon^{\nu_\perp/(2-\eta)} & \text{for } \epsilon > 0 \end{array} \qquad (23)$$

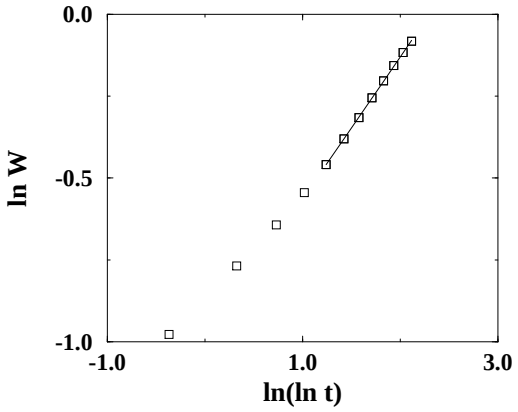

FIG. 7. Width at criticality as a function of time in the restricted model. The graph is as for Fig. 6 and the system size is $N = 2048$. The best fit through the longer time points (2^6— 2^{13} MCS) has a slope of 0.43.

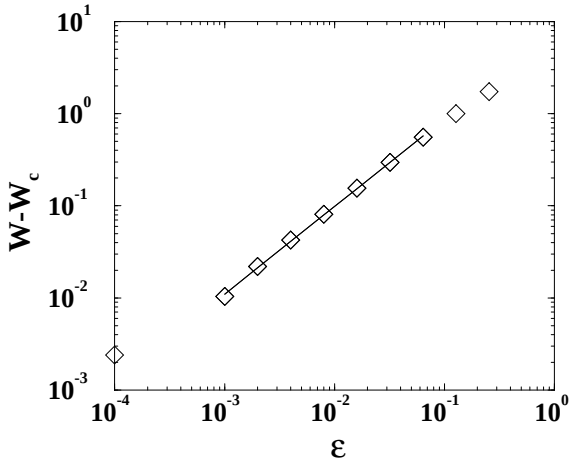

FIG. 8. Double logarithmic plot of width in the moving phase as a function of ϵ. The system size was $N = 512$ and each point is an average over 2000 simulations. The simulations were started from a flat interface and allowed to saturate over 2^{13} MCS. The width was then averaged over another 2^{13} MCS. The straight line corresponds to $\chi = 0.95$. Simulations of the restricted model yielded a similar behavior and estimated exponent value $\chi = 0.92$

We now proceed to examine the actual behavior of the width at criticality. In Figs. 6–7, width against time is plotted for simulations run at criticality. For both unrestricted and restricted models a long time scaling behavior emerges before the width saturates due to the finite length of the system. For times shorter than the saturation time, the width at criticality, W_c, grows as

$$W_{\rm c} \sim (\ln t)^{\gamma} \,. \tag{24}$$

Now since the saturation time is expected to scale as N^z, where z is the dynamic exponent, one deduces that the saturation scaling of the width is

$$W_{\rm c} \sim (\ln N)^{\gamma} \,, \tag{25}$$

where γ is given by $\gamma \simeq 0.24 \approx 1/4$ for the unrestricted model and $\gamma \simeq 0.43$ for the restricted model. These numerical results suggest that the critical exponent η in Eq. (23) is in fact equal to zero. For the restricted model the scaling of the width at criticality is similar to that of an *unrestricted* polynuclear growth model [9] where $\gamma = 1/2$. The relationship between the present models and PNG models will be discussed in Sec. VIII. However, for the unrestricted model the value of γ is clearly distinct from 1/2 which shows that the critical width could display non-universal behavior. On the other hand γ could be restricted to a finite number of possible values. It should also be noted that in preliminary simulations the value of γ was erroneously assumed [17].

We now examine how the saturation width diverges as the growth rate is increased and the interface enters the moving phase. To do this it is convenient to subtract out the critical width and measure $\Delta W(\epsilon) = W(\epsilon) - W_{\rm c}$. Since W_c is negligibly small as compared with $W(\epsilon)$ for $\epsilon > 0$ one expects W and ΔW to have the same asymptotic behavior. In Fig. 8 it is seen that the scaling behavior is

$$\Delta W(\epsilon) \sim \epsilon^{\chi} \,, \tag{26}$$

where $\chi = 0.95(5)$ for the unrestricted model.

This result for χ disagrees with the naive scaling picture (23) which suggests that the width should diverge with the exponent $\nu_\perp/2 = 0.55$ (given that η was found to be equal to zero). We are left to conclude that a more complex behavior than simple scaling takes place.

D. Length Scales in the Moving Phase

In the previous subsection we saw that a simple scaling argument involving only the DP scaling length does not describe correctly the numerical results. In this subsection the aim is to identify possible additional length scales and indicate that complex critical behavior may be present. Therefore the subsection is by nature speculative.

We investigate scaling lengths of the first few layers in the moving phase. We consider the correlation functions $\langle m_k(i) m_k(i+r)\rangle$ of the integrated densities m_k (22) between sites i and $i + r$.

Let us first consider the bottom layer density $m_0 = n_0$. In the *smooth* phase it has already been noted the dynamics of the bottom layer (of the unrestricted model) is exactly that of DP in the active phase. However, in

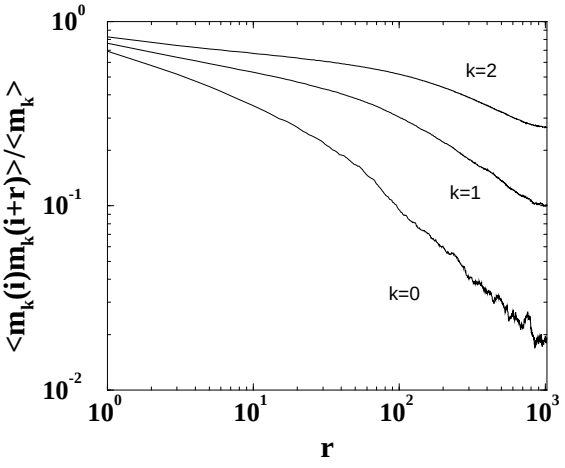

FIG. 9. Correlation functions $\langle m_k(i)m_k(i+r)\rangle/\langle m_k\rangle$ in the moving phase in the unrestricted model. The system parameters are $N = 2048$, $\epsilon = 0.02$ and the results are an average over 1000 simulations each run for 2^{16} MCS to equilibrate.

the *moving* phase there is a subtle difference between the present model and DP in the absorbing phase. This difference stems from the fact that in the present model there is no absorbing state. Instead, whenever a layer is completed the next highest layer becomes the bottom layer. We effectively move in a frame co-moving with the lowest uncompleted layer and relabel the layers appropriately.

In order to show that this produces a non-trivial effect we plot $\langle m_k(i)m_k(i+r)\rangle/\langle m_k\rangle$ in Fig. 9. First recall that in the DP absorbing phase near criticality one expects to see a power law decay $\langle n_0(i)n_0(i+r)\rangle/\langle n_0\rangle \sim \langle m_0(i)m_0(i+r)\rangle/\langle m_0\rangle \sim r^{-\beta/\nu_\perp}$ of the correlation function up to a scaling length which diverges as $\epsilon^{-\nu_\perp}$. At lengths longer than the scaling length the correlation function should decay exponentially with r. In Fig. 9 for $k = 0$ we see an initial power law decay with power given by -0.27, then a crossover at $r \sim \xi_\perp$ to a new power law decay with power $\simeq -0.76$ (rather than to an exponential decay as would be the case with usual DP scaling). We checked for different system sizes and values of ϵ that this qualitative behavior (crossover to a new power law at long distance) was reproduced. Also on Fig. 9 correlation functions for the integrated densities at higher levels are plotted and again one sees crossovers between two power laws. The two powers appear distinct for each level k. For $k = 1$ the two powers are 0.15,0.56 and and for $k = 2$ the two powers are 0.09,0.36. It appears that the crossovers occur at a length dependent on k although it is difficult to quantify this. If the crossover lengths were k dependent then it would imply different length scales existing on different levels

In order to give a heuristic explanation for the above behavior let us consider the density at the bottom layer $m_0 = n_0$. A picture that could explain the crossover phenomena in Fig. 9 is that the sites at the bottom level are grouped into clusters. Each cluster displays the scaling behavior of an active DP cluster and therefore is of typical size $\epsilon^{-\nu_\perp}$ and within a cluster the correlation function decays as $\sim r^{-\beta/\nu_\perp}$. Thus the correlations within clusters generate the first power law decay. However, one also has correlations between clusters. Thus within the cluster picture the second power law measures the decay of correlations between clusters.

A similar cluster picture could hold for the first and second layers $k = 1, 2$. Within the picture, the sites at the first level, for example, are distributed in clusters. The first power law in the $k = 1$ curve of Fig. 9 measures the correlation within a cluster and the second measures correlations between clusters. The fact that the crossover appears to occur at a different distance r than for the bottom layer indicates that the clusters at the first level are larger than those at the bottom level. Therefore there is more than one length scale in the problem.

This picture is far from being complete or verified unambiguously and many questions remain open. For example it is not clear whether the second power laws in Fig. 9 continue indefinitely or are cut off at some larger length. The numerical value of χ is also not explained.

E. Summary of the Scaling Picture

For the sake of clarity we summarize the scaling results of this section and the partial picture of scaling. First we have the smooth phase with exponents x_k associated with the density at each level. x_0 is given by the DP exponent β whereas x_k for $k \geq 1$ appear to be non-trivial, in the sense that they are not simply related to DP exponents. The simple approximation of Sec. IV A gives the qualitative trend but is ruled out quantitatively by the numerics. As the roughening transition is approached the DP scaling length $\xi_\perp$ and scaling time $\xi_\parallel$ hold at all levels. This implies that approaching the transition the dynamic exponent is $z = \nu_\parallel/\nu_\perp$.

At the transition the interface has logarithmically diverging width of the form (25). However the value of γ appears to depend on which version of the model one simulates. This could either point to γ being non-universal or that it can take one of a finite number of values.

Above the transition the velocity grows with the DP exponent $\nu_\parallel$. This reflects presence of the DP scaling length and time at the bottom level. However by measuring the growth of the interface width we have ruled out a simple scaling picture involving only the DP scaling length. We have provided evidence to suggest that there may be longer scaling lengths which characterize the size of clusters of sites at higher levels. This picture remains to be fully investigated. Likewise the question of scaling times for different levels in the rough phase has not been fully addressed. (In the rough phase the dynamic

exponent should take the KPZ value $z = 3/2$).

It is interesting to note that in a very recent renormalization group analysis of the field theory introduced in Sec. VII, multicritical behavior was identified [32]. This could be consistent with the complicated scaling behavior we have observed.

V. SPONTANEOUS SYMMETRY BREAKING

The growth models defined in Sec. II may be viewed as examples of spontaneous symmetry breaking (SSB) in a 1d system with periodic boundary conditions and a non-conserved order parameter. As will be shown, the models display a robust local mechanism for eliminating islands of the minority phase generated by fluctuations.

The symmetry of the growth models, apart from spatial translation and reflection invariance, is a (discrete) translational invariance in the heights (Z_∞). In the smooth phase this symmetry is broken since the system spontaneously selects one of the heights as a reference level which then serves as bottom layer for local fluctuations of the smooth interface.

A. Order parameters.

In order to quantify the symmetry breaking, we define a magnetization-like order parameter (valid for both the restricted and the unrestricted models):

$$M_1 = \frac{1}{N}\sum_{j=1}^{N}(-1)^{h_j}\,. \tag{27}$$

This order parameter is clearly not conserved by the dynamical rules of the models. In the smooth phase $q < q_c$, it has a nonvanishing expectation value $\langle M_1\rangle \neq 0$ in the thermodynamic limit where $\langle\ldots\rangle$ denotes thermal average. On the other hand, in the rough phase the interface explores many height levels therefore the contribution to the magnetization at different sites are uncorrelated over long distances and $\langle M_1\rangle = 0$. Near the phase transition we expect the order parameter to vanish as

$$\langle M_1\rangle \sim |\epsilon|^{\theta_1}\,, \tag{28}$$

where θ_1 is the associated critical exponent.

The order parameter and the SSB mechanism are illustrated in Fig. 10. Here the heights are represented by alternating black and white coloring (c.f. Fig. 1) and therefore the average greyscale in the figure is related to the magnitude of M_1. Also it is shown how a large island of one phase shrinks when introduced into a system dominated by the other phase, thus ensuring the stability of the smooth phase. This behavior is typical of islands of all sizes, except for those extending over the whole system.

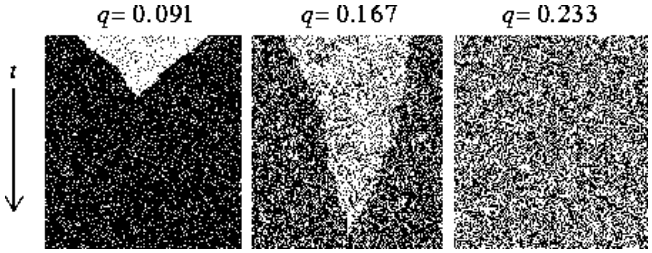

FIG. 10. MC simulation of the restricted model for a systems of size 600 at different values of q. Each configuration is a row of pixels, with sites at even (odd) heights represented by black (white) pixels, visualizing the order parameter M_1. Configurations at intervals of 7 moves per site are shown up to 2100 sweeps. Initially, a large island of size 400 is introduced. For $q < q_c$, the island shrinks and disappears, illustrating the mechanism that insures long-range order in the smooth phase. The typical time it takes for the island to disappear depends on q, it increases and finally diverges when $q \to q_c$. Similarly the magnitude of the order parameter M_1 (visualized by the greyscale contrast between the two phases) decreases. At criticality the order parameter is zero so that the island is not visible any more.

	θ_1	θ_2	θ_3	θ_4	θ_5
unrestricted:	0.64(3)	0.40(2)	0.24(2)	0.15(1)	0.11(1)
restricted:	0.66(6)	0.37(4)	0.21(4)	0.14(3)	0.10(2)

TABLE II. Numerical estimates for the order parameter exponents θ_k obtained from dynamic MC simulations.

Since the symmetry of the model in the heights is Z_∞, we can define a family of order parameters which generalize M_1:

$$M_n = \left|\frac{1}{N}\sum_{j=1}^{N}\exp\Big(\frac{2\pi i\, h_j}{n+1}\Big)\right|\,. \tag{29}$$

These order parameters have the same qualitative behavior as M_1 and can be understood as discrete Fourier transforms of the height probability distribution. It turns out that each order parameter is characterized by a different critical exponent:

$$\langle M_n\rangle \sim |\epsilon|^{\theta_n}\,. \tag{30}$$

As in the case of the density exponents x_k, we determined the exponents θ_n numerically by static, finite-size and dynamic MC simulations. The most precise data are obtained from dynamic simulations (see Fig. 11). The numerical estimates for θ_k are summarized in Table II. It seems that these exponents are non-trivial in the sense that they cannot be related in a simple manner by scaling relations to the known DP exponents.

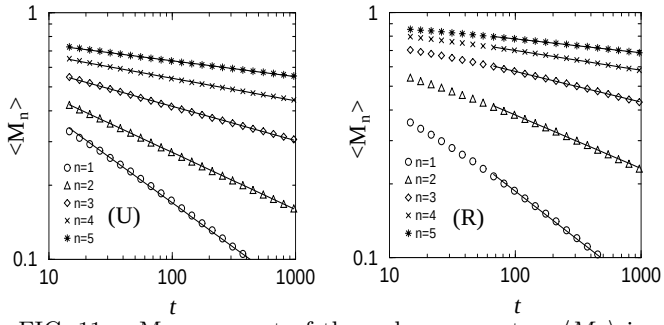

FIG. 11. Measurement of the order parameters $\langle M_n \rangle$ in dynamic MC simulations for (U) the unrestricted and (R) the restricted variant of the growth model.

B. External ordering fields.

For each order parameter M_n one can define a conjugate ordering field that favors states where the order parameter is positive. This ordering field can be introduced by a periodic modulation of the growth rate, *i.e.* we replace the uniform growth rate q by a height-dependent growth rate

$$q \to q(h_i) = q - \lambda \cos\Big(\frac{2\pi\, h_i}{n+1}\Big)\,, \tag{31}$$

where λ is the magnitude of the ordering field. For example, for $n = 1$ and $\lambda > 0$ the growth on the bottom layer and other even layers is penalised whereas growth on odd layers is favored. At criticality, the response to this external field is expected to obey a power-law behavior

$$M_n \sim \lambda^{\kappa_n}\,. \tag{32}$$

We measured the exponents κ_n in static MC simulation at criticality (see Fig. 12). Varying λ over two decades from 10^{-3} to 10^{-1} we obtain the estimates $\kappa_1 = 0.60(4)$, $\kappa_1 = 0.42(3)$, $\kappa_1 = 0.26(3)$, $\kappa_1 = 0.17(3)$, and $\kappa_1 = 0.12(3)$. Comparision with the results in Table II suggest that $\kappa_n = \theta_n$.

C. Spontaneous breaking of continuous symmetries.

So far we have shown that the growth models discussed in this paper exhibit spontaneous breaking of a *discrete* symmetry in one dimension. It is therefore of interest to ask whether a *continuous symmetry* can also be broken in one-dimensional nonequilibrium models. Continuous symmetries, where the order parameter can take a continuum of values, seem to be harder to break than discrete symmetries. Consider for example the equilibrium case: discrete symmetries can be broken above one dimension; continuous symmetries, however, can be broken only above two dimensions, although weaker vortex ordering transitions are possible in 2d (Kosterlitz-Thouless transitions [29]).

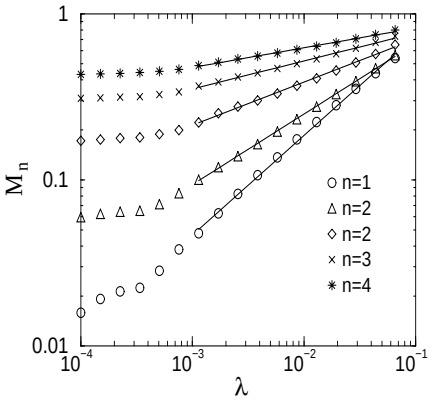

FIG. 12. Response of the order parameter M_1 to an external ordering field at the critical point in the unrestricted model with 2000 sites. Measuring the slope of the line in the double-logarithmic plot over two decades gives estimates for the response exponents κ_n (see text). The saturation for very low values of λ seems to be a finite-size effect.

Here we present a version of the growth model with a continuous symmetry which is broken spontaneously in the smooth phase. The only difference between this version and the unrestricted model described above is that the height increment at a growth move is a continuous rather than a discrete number.

The model is defined on a 1d lattice with periodic boundary conditions and continuous (real) height variables h_i at sites $i = 1 \ldots N$. The interface evolves by choosing a site i at random and carrying out one of the processes

$$\begin{aligned} h_i &\to h_i + \zeta && \text{with probability } q \\ h_i &\to \min(h_i, h_{i+1}) && \text{with probability } (1-q)/2 \\ h_i &\to \min(h_i, h_{i-1}) && \text{with probability } (1-q)/2 \end{aligned} \tag{33}$$

where ζ is a positive real random number selected from a flat distribution between 0 and 1. The symmetry of this model (apart from spatial translations and reflections) is continuous translational invariance in the heights, i.e. overall shifts of the interface heights by any amount. The symmetry breaking corresponds to the fact that in the smooth phase the interface selects a given height which is a real number, and remains pinned to that height for a time that grows exponentially with the system size.

Starting from a flat interface at height zero, the dynamics taking place at the lowest level in the continuous model are exactly the same as in the unrestricted version of the discrete model, the simple reason being that in both cases each height level is decoupled from the higher ones. This means that both models have the same critical point $q_c = 0.23267(3)$. Moreover, they have the same occupation of the lowest level which is characterized by $n_0 = (q_c - q)^{x_0}$ where $x_0 = \beta \simeq 0.277$ is the DP density exponent.

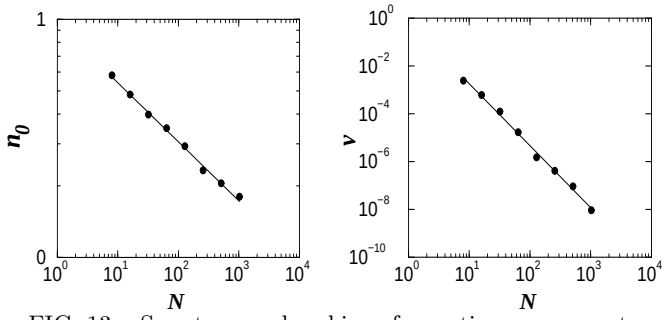

FIG. 13. Spontaneous breaking of a continuous symmetry: The graphs show the occupation of the bottom layer n_0 and the growth velocity v in a system of size N at criticality. From the slopes we obtain the exponents $x_0/\nu_\perp = 0.245(10)$ and $y/\nu_\perp = 2.59(7)$.

Above the critical point, the interface is rough and has a finite growth velocity. Simulations show that the roughness exponent characterizing the interface at this phase is consistent with the KPZ exponents [2], within numerical accuracy. However, an interesting difference from the discrete model occurs in the growth velocity v. As in the previous case, it is related to the inverse of the island lifetime. However in the present case, the step size by which the interface grows is not 1, but rather a real random number between 0 and 1. Each completed layer corresponds to the growth of the interface by the smallest surviving step. Now, from our results on the discrete models we expect that at criticality the width behaves as some power of $\ln N$. Since the number of steps in a finite system is of the order of N, we expect the smallest of them to be of order $1/N$. At the critical point, therefore, we expect the following finite size scaling for the velocity

$$v \sim N^{-\nu_{||}/\nu_\perp - 1} \tag{34}$$

which corresponds to the scaling

$$v \sim (q - q_c)^y \,, \qquad y = \nu_{||} + \nu_\perp \simeq 2.83 \,. \tag{35}$$

This has to be compared with $y = \nu_{||} \simeq 1.73$ in the discrete model. These exponents are in good agreement with the values measured in MC simulations, as shown in Fig. 13. It would be interesting to study order parameters M_ω which are continuous generalizations of M_n in Eq. (29):

$$M_\omega = \left| \frac{1}{N} \sum_{j=1}^{N} \exp(2\pi i \omega\, h_j) \right| . \tag{36}$$

As before, we expect a power law behavior $\langle M_\omega \rangle \sim |\epsilon|^{\theta(\omega)}$ where $\theta(\omega)$ depends continuously on ω.

VI. MEAN FIELD APPROXIMATION

In this section we derive the mean field equations corresponding to the model (1)–(3) and study the resulting steady state distribution. We consider the unrestricted SOS model since the equations for this case are somewhat simpler. However, both the restricted and the unrestricted models are expected to exhibit the same qualitative dynamical behavior.

To derive the mean field equations we introduce at each site i a set of variables $\psi_k(i)$, $k = 0, ..., \infty$. Here $\psi_k(i)$ is equal to 1 if the interface at site i is at height k and it is equal to 0 otherwise. Let $\langle \psi_k(i) \rangle$ be the average of $\psi_k(i)$ over all realizations of the dynamical equations starting with the same initial configuration. Let us first consider the occupation of the zeroth level. The adsorption and desorption processes defined in Eqs. (1)–(3) result in the following equation for $\langle \psi_0(i) \rangle$:

$$\begin{aligned} \Lambda \frac{\langle \partial \psi_0(i) \rangle}{\partial t} = & -q \langle \psi_0(i) \rangle \\ & + \frac{1}{2}(1-q) \langle \psi_0(i)(1 - \psi_0(i-1) \rangle \\ & + \frac{1}{2}(1-q) \langle \psi_0(i)(1 - \psi_0(i+1) \rangle \,, \end{aligned} \tag{37}$$

where Λ is a time constant, which, for simplicity, may be taken as $1 - q$. Within the mean field approximation, one replaces the correlation function $\langle \psi_0(i)\psi_0(j) \rangle$ by the product $\langle \psi_0(i) \rangle \langle \psi_0(j) \rangle$. For the ring geometry considered in this work $\langle \psi_0(i) \rangle$ is independent of the site index i. Denoting $\langle \psi_0(i) \rangle$ by ρ_0 we obtain the following dynamical equation for ρ_0

$$\frac{\partial \rho_0}{\partial t} = -\bar{q}\rho_0 + \rho_0(1 - \rho_0) \,, \tag{38}$$

where $\bar{q} = q/(1-q)$. Similar considerations yield the following set of equations for $\rho_k = \langle \psi_k(i) \rangle$ for $k \geq 1$:

$$\frac{\partial \rho_k}{\partial t} = \bar{q}\rho_{k-1} - \bar{q}\rho_k + \rho_k \left(1 - \sum_{j=0}^{k} \rho_j \right) - \rho_k \sum_{j=0}^{k-1} \rho_j \,. \tag{39}$$

It is convenient to rewrite Eqs. (38),(39) in terms of the integrated density variables (c.f. Eq. (22))

$$\phi_k = \sum_{j=0}^{k} \rho_j \,. \tag{40}$$

Substituting (40) and using $\rho_k = \phi_k - \phi_{k-1}$ brings (38),(39) into the form

$$\begin{aligned} \frac{\partial \phi_0}{\partial t} &= \epsilon \phi_0 - \phi_0^2 \\ \frac{\partial \phi_k}{\partial t} &= \epsilon \phi_k - \phi_k^2 + (1-\epsilon)\phi_{k-1} \quad (k \geq 1) \,, \end{aligned} \tag{41}$$

where $\epsilon = 1 - \bar{q}$. These equations have a stationary solution corresponding to a smooth interface for $\epsilon > 0$. The roughening transition takes place at $\epsilon = 0$. The

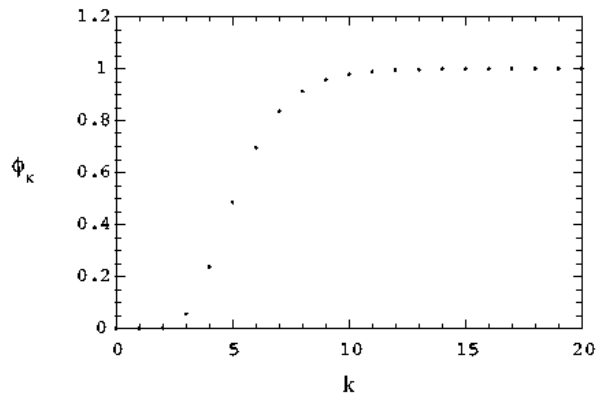

FIG. 14. Mean field approximation of the integrate height density ϕ_k at level k.

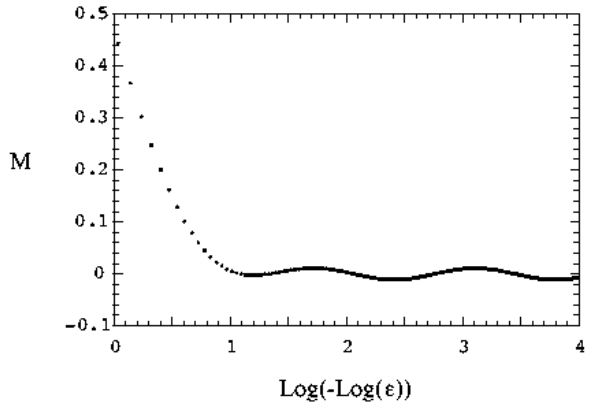

FIG. 15. Mean field approximation of the magnetization M_1 as a function of $\ln[-\ln(\epsilon)]$.

stationary solution for $\epsilon > 0$ may be calculated by tl following recursion relation:

$$\phi_k = \frac{1}{2}\left[\epsilon + \sqrt{\epsilon^2 + 4(1-\epsilon)\phi_{k-1}}\,\right] \qquad (4$$

with $\phi_0 = \epsilon$. To leading order in ϵ Eq. (42) takes tl form

$$\phi_k = \sqrt{\phi_{k-1}}\,. \qquad (43)$$

The steady state distribution corresponding to this recursion relation is

$$\phi_k = \epsilon^{(1/2)^k}\,. \qquad (44)$$

Therefore the mean field values of the exponents x_k defined in Eq. (7) are given by

$$x_k^{MF} = \frac{1}{2^k}. \qquad (45)$$

The integrated height density ϕ_k is a monotonically increasing function of k, varying from ϵ for $k = 0$ to 1 for $k \to \infty$ (see Fig. 14). It exhibits a rapid increase near $k \simeq k_m$ which is determined by the following equation:

$$\phi_{k_m-1} + \phi_{k_m+1} - 2\phi_{k_m} = 0\,. \qquad (46)$$

The index k_m corresponds to the interface height at which the density $\rho_k = \phi_k - \phi_{k-1}$ is maximal. Using Eq. (43) one finds that to leading order in ϵ

$$k_m \approx \frac{1}{\ln 2}\ln[-\ln(\epsilon)]\,. \qquad (47)$$

It is easy to see that the width of the ϕ distribution remains finite even in the limit $\epsilon \to 0$. The interval Δk corresponding to a change of ϕ from some value ϕ_{min} to another, say, ϕ_{max} is given to leading order in ϵ by

$$\Delta k = \frac{1}{\ln 2}\ln[\ln(\phi_{min})/\ln(\phi_{max})]. \qquad (48)$$

This interval is independent of ϵ, and thus the width of the ϕ_k distribution is *finite*. This feature, together with Eq. (47) yield the following behavior for the average height :

$$\langle h\rangle \sim \sqrt{\langle h^2\rangle}\ \sim \ln[-\ln(\epsilon)] \qquad (49)$$

We now turn to the magnetization-like order parameter $M_1 = \sum_j (-1)^j \rho_j$ (see Eq. (27)). For small $\epsilon > 0$ Eq. (44) yields the following expression for M_1

$$M_1 = \epsilon + \sum_{k=1}^{\infty} \epsilon^{(1/2)^k}(1 - \epsilon^{(1/2)^k})(-1)^k\,. \qquad (50)$$

In Fig. 15 we plot the magnetization as a function of $\ln(-\ln(\epsilon))$. It is readily seen that M_1 does not decay to zero for small ϵ. Rather it oscillates with an amplitude which remains finite at small ϵ. This may easily be understood in the following way: the main contribution to the sum (50) comes from a finite number of layers centered around $k = k_m$. As ϵ decreases, k_m increases, and the magnetization order parameter probes different layers. Since the contributions of the layers have alternate signs, the magnetization becomes oscillatory. This feature is an artifact of the mean field approximation. In this approximation fluctuations of the position of the interface are neglected. When they are taken into account they are expected to broaden the interface, resulting in a diverging width at the roughening transition. This should lead to a vanishing magnetization at the transition. In a similar fashion, the mean field theory of KPZ interfaces does not describe the roughening behavior.

VII. FIELD THEORY

In order to understand the universal properties observed in the growth models at criticality, it is useful to study the corresponding field theory. As will be explained below, such a field theory describes a hierarchy

of unidirectionally coupled DP processes. Thus it should play a role in even more general contexts, namely whenever DP-like processes are coupled unidirectionally *without* feedback.

Unlike the KPZ equation [2], the field theory we consider involves separate fields for each height level in order to incorporate the rule that atoms cannot desorb from the middle of an island. Let us first try to guess the Langevin equations by adding appropriate diffusion and noise contributions such that (a) the equation for the lowest level reproduces the ordinary Langevin equation for directed percolation [30], (b) at a given time and position the sum over all height densities $\sum_k \rho_k$ is equal to one, and (c) the hierarchy of equations is translational invariant in space and time as well as in the heights. The simplest set of Langevin equations that meets these requirements reads (suppressing the arguments x, t)

$$\partial_t \rho_0 = -\bar{q}\rho_0 + \rho_0(1-\rho_0) + \nabla^2\rho_0 + \eta_0 \tag{51}$$

$$\begin{aligned}\partial_t \rho_k = \bar{q}\rho_{k-1} - \bar{q}\rho_k + \rho_k\Big(1 - \sum_{i=0}^{k}\rho_i\Big) - \rho_k \sum_{i=0}^{k-1}\rho_i \\ +\nabla^2\rho_k - \nabla^2\rho_{k-1} + \eta_k - \eta_{k-1} \quad (k>1)\,,\end{aligned} \tag{52}$$

where $\eta_k(x,t)$ are field-dependent Gaussian noise fields with two point correlations to be specified below. Notice that Eq. (51) is just the ordinary Langevin equation for DP [30]. One can also verify that the sum over all density fields $\sum_{k=0}^{\infty}\rho_k$ is a constant of motion.

As in the previous section, these equations can be simplified by introducing integrated density fields $\phi_k(x,t) = \sum_{j=0}^{k}\rho_j(x,t)$, resulting in

$$\partial_t\phi_k = a\phi_k - \phi_k^2 + \bar{q}\phi_{k-1} + \nabla^2(\phi_k - \phi_{k-1}) + \eta_k\,, \tag{53}$$

where $a = 1-\bar{q}$ and $\phi_{-1} = 0$. Interestingly, the introduction of integrated densities also led to a considerable improvement of the numerical results in Sect. IV, suggesting that these quantities are more natural in the context of the present problem than the height densities $\rho_k(x,t)$.

Although the Langevin equations (53) follow quite naturally from the principles (a)-(c) stated above, it can be dangerous to conjecture the correlations of the noise fields $\eta_k(x,t)$. A systematic derivation of the Langevin equations and the noise correlations based on a bosonic operator formalism [31] will be presented in Ref. [32]. Dropping irrelevant operators (like $\nabla^2\phi_{k-1}$ in Eq. (53)) and introducing independent coefficients for all terms it is shown that the Langevin equations are given by

$$\partial_t\phi_k = a_k\phi_k - \lambda_k\phi_k^2 + \bar{q}_k\phi_{k-1} + D_k\nabla^2\phi_k + \eta_k \tag{54}$$

with noise correlations

$$\langle\eta_k(x,t)\eta_l(x',t')\rangle = 2\Gamma_{k,l}\,\phi_k(x,t)\,\delta(x-x')\,\delta(t-t')\,, \tag{55}$$

where $k<l$. Notice that there are noise correlations *between* different height levels k,l which are generated in a one-loop approximation by non-trivial mixed cubic vertices [32].

In Sect. IV we observed numerically that the scaling exponents $\nu_\perp$ and $\nu_{||}$ are identical on all height levels. This observation can be verified easily within an 'improved mean field approximation' as follows. Consider the scaling transformation

$$x \to \Lambda x\,, \quad t\to\Lambda^z t\,, \quad \phi_k \to \Lambda^{-\chi_k}\phi_k\,, \tag{56}$$

where z is the dynamical exponent and χ_k are the scaling exponents of the fields ϕ_k. Under rescaling, Eqs. (54) and (55) turn into

$$\begin{aligned}\partial_t\phi_k = a_k\Lambda^z\phi_k - \lambda_k\Lambda^{z-\chi_k}\phi_k^2 \\ +\bar{q}_k\Lambda^{z+\chi_k-\chi_{k-1}}\phi_{k-1} + D_k\Lambda^{z-2}\nabla^2\phi_k + \eta_k'\,,\end{aligned} \tag{57}$$

$$\begin{aligned}\langle\eta_k'(x,t)\eta_l'(x',t')\rangle = 2\,\Lambda^{z+\chi_l-d}\,\Gamma_{k,l}\,\phi_k(x,t) \\ \times\delta(x-x')\,\delta(t-t')\,, \qquad (k<l)\end{aligned} \tag{58}$$

where d is the spatial dimension. Thus an infinitesimal rescaling by $\Lambda = 1+m$ would result in a change of the coefficients

$$\begin{aligned}\partial_m\, a_k &= a_k\, z \\ \partial_m\,\lambda_k &= \lambda_k\,(z-\chi_k) \\ \partial_m\, D_k &= D_k\,(z-2) \\ \partial_m\,\Gamma_{k,l} &= \Gamma_{k,l}\,(z+\chi_l-d) \\ \partial_m\,\bar{q}_k &= \bar{q}_k\,(z+\chi_k-\chi_{k-1})\end{aligned} \tag{59}$$

At the critical dimension $d = d_c$, we expect the coefficients to be invariant under rescaling. As usual, the DP equation at the lowest level $k=0$ yields the solution $z=2$, $\chi_0 = 2$, and $d_c = 4$. The linear term is relevant so that the parameter a_0 has to be tuned to zero (this is the mean-field critical point of DP). Also at higher levels $k>0$ the linear term is the most relevant contribution wherefore $a_k = 0$ is the multicritical point in mean-field. Requiring that the nonlinearity and the coupling to the previous level are equally relevant ($z+\chi_k-\chi_{k-1} = z-\chi_k$), we are led to the solution $\chi_k = 2^{1-k}$. Identifying $z = \nu_{||}/\nu_\perp$ and $\chi_k = x_k/\nu_\perp$ we obtain, in agreement with Sec. VI, the mean field exponents

$$\nu_{||}^{MF} = 1\,, \qquad \nu_\perp^{MF} = \frac{1}{2}\,, \qquad x_k^{MF} = \frac{1}{2^k}\,. \tag{60}$$

The field theory (54)-(55) may be interpreted as a hierarchy of DP processes which are *unidirectionally* coupled by the term $\bar{q}_k\phi_{k-1}$. Identifying the fields $\phi_0, \phi_1, \phi_2, \ldots$ with densities of particles $A, B, C, \ldots$, this field theory corresponds to the reaction-diffusion process

$$\begin{aligned} A &\leftrightarrow 2A\,, \quad A\to B \\ B &\leftrightarrow 2B\,, \quad B\to C \\ C &\leftrightarrow 2C\,, \quad C\to D \\ &\ldots \qquad\quad \ldots\end{aligned}$$

MC simulations indicate that this reaction-diffusion process belongs indeed to the same universality class as the roughening transition discussed in this paper. We therefore expect that this field theory describes not only the present growth models but any system in which DP processes are coupled in one direction.

VIII. RELATION TO POLYNUCLEAR GROWTH MODELS

In the previous sections we have seen that the dynamics of the lowest layer undergoes a DP transition that corresponds to a transition from zero to finite velocity of the interface. For a class of models termed Polynuclear Growth (PNG) [6,7,9,15,16], which employ *parallel* dynamics, a similar scenario pertains to the growth at the highest level. In these models the use of parallel dynamics implies that the maximum velocity is 1 *i.e.* the sites at the highest level $h = T$ grow at every time step T. The sites at the highest level may be considered as active sites of a DP process and below the transition there is a non-zero density of such sites. Above the transition there are no sites at the highest level and the velocity is less than 1. This transition is lost, however, when the dynamics are performed random-sequentially since then there is no maximum velocity. This contrasts with the model (1)–(3) where a phase transition is found whether the dynamics be implemented random-sequentially or in parallel.

In this section we shed some light on the connection between the present models and models of the PNG class. In order to do this we first generalize the dynamics of the unrestricted model (1)–(3) to encompass both random sequential and parallel dynamics. In a time step *all* sites are updated according to the following rule:

$$\begin{aligned} & h_i(T+1) \\ & = h_i(T) \ \text{ with prob.} \quad 1-\Delta \\ & = h_i(T)+1 \ \text{ with prob.} \quad q\Delta \\ & = \min\left[h_i(T), h_{i+1}(T)\right] \ \text{ with prob.} \quad (1-q)\Delta/2 \\ & = \min\left[h_{i-1}(T), h_i(T)\right] \ \text{ with prob.} \quad (1-q)\Delta/2 \end{aligned} \tag{61}$$

As Δ varies from 0 to 1, the rule (61) interpolates between random sequential dynamics and parallel dynamics: for $\Delta \ll 1/N$ the height of at most one site is modified at any time step and the dynamics becomes random sequential; for $\Delta = 1$ all sites are modified at each time step and the dynamics is parallel.

We now make a transformation suggested to us by J. Krug (private communication). If one defines

$$h_i(T) = T - g_i(T)\ , \tag{62}$$

the variables $g_i(T)$ undergo the following dynamics:

$$\begin{aligned} & g_i(T+1) \\ & = g_i(T)+1 \ \text{ with prob.} \quad 1-\Delta \\ & = g_i(T) \ \text{ with prob.} \quad q\Delta \\ & = \max\left[g_i(T), g_{i+1}(T)\right]+1 \ \text{ with prob.} \quad (1-q)\Delta/2 \\ & = \max\left[g_{i-1}(T), g_i(T)\right]+1 \ \text{ with prob.} \quad (1-q)\Delta/2\ . \end{aligned} \tag{63}$$

The rules (63) yield a growth model where the maximum velocity is 1 and the DP transition appears at the maximal height level, as occurs with PNG models. However, it is important to note that the dynamics (63) is always parallel in nature since the heights of many sites are modified at each time step. Thus both random sequential and parallel versions of (61) are mapped onto a parallel rule (63).

We now compare (63) with a specific PNG model studied in [9]. In that model the heights of a $1d$ interface are updated in parallel in two sub-steps. First all up (down) steps of the interface move deterministically to left (right) a distance of u lattice spacings. Then all heights are incremented by 1 with probability p. (For our purposes it is convenient to group the two substeps in the reverse order to that of [9] but this does not change the dynamics). Thus the model is unrestricted. For the case $u = 1$ this dynamics may be written as a single parallel update where

$$\begin{aligned} & g_i(T+1) \\ & = \max\left[g_{i-1}(T), g_i(T), g_{i+1}(T)\right]+1 \ \text{ with prob.} \quad p \\ & = \max\left[g_{i-1}(T), g_i(T), g_{i+1}(T)\right] \ \text{ with prob.} \quad (1-p)\ . \end{aligned} \tag{64}$$

Clearly the two dynamics (63),(64) are similar in character but distinct. Furthermore in [9] it was found that at $p_c \simeq 0.527$ the width of the interface scales as $W \sim (\ln N)^{1/2}$ which is distinct from the behavior of the unrestricted model but similar to that of the *restricted model* of the present paper.

In this section we have seen a subtle connection between the growth models studied in the present paper and models similar in character to PNG models. This was done by generalizing the dynamics of the present model to a dynamics that interpolates between random sequential and parallel. Then, transforming the present model via (62) one obtains a model with parallel dynamics which has similarities with, but is distinct from, the PNG models previously studied. However, with the standard PNG model (64) the dynamics is strictly parallel and it is not clear if it can be transformed to any random sequential model. Indeed, simply employing the inverse transform of (62) yields another model with strictly parallel dynamics.

IX. CONCLUSIONS

In summary, we have studied in detail a one-dimensional stochastic growth model with random sequential dynamics that exhibits a transition from a smooth to a rough phase. In studying the model we have

shown that some properties may be understood directly from the scaling behavior of DP. However, other properties and critical exponents appear non-trivial in the sense that they seem not to be related to DP quantities in a simple manner. Furthermore, we have introduced novel exponents such as those relating to the magnetization like order parameters characterizing the SSB and the response of these order parameters to an ordering field.

One can also think of the model in terms of a system of unidirectionally coupled DP processes. We have proposed a field theory which should describe the properties of this general class of systems.

We are left with several open questions. Firstly can the values of the novel exponents be predicted? Secondly can the critical behavior be described by a conventional scaling picture? In our study we have indicated that the critical behavior may be quite complicated. This could be consistent with multicritical behavior found in a study [32] of the field theory proposed in Sec. VII.

We have also made a subtle connection between the present random sequential models and models similar in character to the parallel update PNG models such as that studied in [9]. It would be instructive to explore this point further.

It would also be of interest to study in more detail the model (33) that exhibits the breaking of a continuous symmetry. In particular the order parameter (36) has not been fully investigated.

The growth models and their scaling behavior were investigated in one dimension. However, it is straightforward to define the models in higher dimensions where similar scaling behavior is expected to hold.

Let us finally remark that it would be very interesting to search for experimental realizations of the growth processes discussed in this paper, in particular because of their relation to DP. As pointed out by Grassberger [33], the large body of theoretical work on DP seems to be unbalanced by the fact that there are no experiments where DP exponents have actually been measured. It is not yet clear whether this is due to a lack of such experiments or to an oversimplification of nature in DP models. The growth models, however, suggest another category of experiments where DP exponents may be identified, namely absorption-desorption processes where the evaporation of atoms from the middle of completed layers is highly suppressed.

Acknowledgments: We thank P. Bladon, Y.Y. Goldschmidt, M. J. Howard, J. Krug, V. Rittenberg, P. Sollich, U. C. Täuber and N. B. Wilding for interesting discussions. MRE is a Royal Society University Research Fellow and thanks the Weizmann Institute for warm hospitality during several visits when this work was in progress. UA is supported by a Rothchild Fellowship. This work was supported by Minerva Foundation, Munich, Germany.

APPENDIX A: AN EXACTLY SOLVABLE CASE

It is instructive to consider a case where the steady state can be calculated exactly. This will allow us to verify that the interface is indeed rough in the moving phase and that if we allow some rate for desorption from the middle of a plateau, the interface is rough independent of whether the velocity is positive, negative or zero.

The transition rates we consider are that of the RSOS model presented in the introduction with the addition of a process with rate p.

$$\begin{aligned}
0\,+ &\;\rightarrow\; +\,0 \quad \text{with rate } g\\
+\,0 &\;\rightarrow\; 0\,+ \quad \text{with rate } 1\\
-\,0 &\;\rightarrow\; 0\,- \quad \text{with rate } g\\
0\,- &\;\rightarrow\; -\,0 \quad \text{with rate } 1\\
0\;\;0 &\;\rightarrow\; +\,- \quad \text{with rate } g\\
+\,- &\;\rightarrow\; 0\;\;0 \quad \text{with rate } 2\\
-\,+ &\;\rightarrow\; 0\;\;0 \quad \text{with rate } g\\
0\;\;0 &\;\rightarrow\; -\,+ \quad \text{with rate } p
\end{aligned} \tag{A1}$$

The process with rate p translates to desorption from the middle of a plateau when the model is translated back into a growth model via (11). We shall using a technique similar to that employed recently in [14] (see also [13]) to show that if

$$p = 1 - g/2 \tag{A2}$$

the steady state probabilities P of a configuration may be written in a factorized form

$$P(M) = Z_N^{-1}\; 2^{-M}\,, \tag{A3}$$

where M is the number of positive charges in the configuration and Z_N is a normalization. One also has the constraint that the only allowed configurations have equal numbers of positive and negative charges due to the fact that dynamics conserves the global charge. Taking this into account the normalization Z_N is given by

$$Z_N = \sum_{M=0}^{N/2} \frac{N!}{M!\;M!\;(N-2M)!}\, 2^{-M}\,. \tag{A4}$$

In order to prove Eq. (A3) let us define variables $b_{+0}, b_{++}, b_{+-} \ldots$ where, for example, b_{+0} is the number of bonds $i, i+1$ where there is a positive particle at site i and a hole at site $i+1$. Due to the fact that the global charge is zero we have $b_{+0} + b_{++} + b_{+-} = b_{0+} + b_{++} + b_{-+} = b_{-0} + b_{--} + b_{-+} = b_{0-} + b_{--} + b_{+-} = M$ which leads to

$$b_{+0} + b_{0-} + 2b_{+-} = b_{0+} + b_{-0} + 2b_{-+} \tag{A5}$$

If Eq. (A3) is to hold in the steady state the following equation for the balance of probability must hold for any configuration:

$$
\begin{aligned}
&(b_{+0} + g b_{0+} + b_{0-} + g b_{-0} \\
&+2b_{+-} + g b_{-+} + (g+p) b_{00}) P(M) \qquad \text{(A6)} \\
&= (b_{0+} + g b_{+0} + b_{-0} + g b_{0-}) P(M) \\
&+(2+g) b_{00} P(M+1) + (g b_{+-} + p b_{-+}) P(M-1)
\end{aligned}
$$

To understand Eq. (A6) note that the lhs gives the rate of loss of probability due to the transitions out of the configuration and the rhs gives the rate of gain of probability due to the transitions into the configuration. We now divide through by (A3) and use (A5) in (A6) to yield

$$
(g+p) b_{00} - g b_{-+} = (1 + g/2) b_{00} + (2p-2) b_{-+} \,, \quad \text{(A7)}
$$

which is satisfied for arbitrary b_{00}, b_{-+} when (A2) holds.

In order to calculate the velocity and roughness for N large one notes that the sum for the normalization (A4) is dominated by $M = N\,(1 - 1/\sqrt{2})$, therefore ρ, the steady state density of positive charges (and also that of negative charges), is

$$
\rho = 1 - 1/\sqrt{2} + \mathcal{O}(1/N) \,. \qquad \text{(A8)}
$$

Here we define the velocity v as the steady state growth rate at an arbitrary site i. Let $\langle c_i c_{i+1} \rangle$ be the steady state expectation of finding a charge c_i at site i and a charge c_{i+1} at site $i+1$, then

$$
\begin{aligned}
v = {} & g \langle 0_i \, +_{i+1} \rangle - \langle +_i \, 0_{i+1} \rangle \\
& - \langle 0_i \, -_{i+1} \rangle + g \langle -_i \, 0_{i+1} \rangle \\
& + (3g/2 - 1) \langle 0_i \, 0_{i+1} \rangle \\
& - 2 \langle +_i \, -_{i+1} \rangle + g \langle -_i \, +_{i+1} \rangle \,. \qquad \text{(A9)}
\end{aligned}
$$

The form (A3) implies that correlation functions factorize to leading order in $1/N$ (e.g. $\langle +_i \, +_{i+1} \rangle \simeq \rho^2$) and one finds

$$
\begin{aligned}
v &= 2(g-1)\rho(1-2\rho) \\
&\quad + (3g/2 - 1)(1-2\rho)^2 + (g-2)\rho^2 + \mathcal{O}(1/N) \\
&\simeq (2 - \sqrt{2})(g-1) \,. \qquad \text{(A10)}
\end{aligned}
$$

One can also calculate the roughness exactly. First we define the height at site i relative to site N as

$$
h_i = \sum_{j=1}^{i} c_j \,. \qquad \text{(A11)}
$$

Clearly $\langle h_i \rangle = 0$, therefore the width w is defined through

$$
w^2 = \frac{1}{N} \sum_{i=1}^{N} \langle h_i^2 \rangle \,. \qquad \text{(A12)}
$$

A moderate calculation then yields

$$
w^2/N = \rho/3 + \mathcal{O}(1/N) \simeq (1 - 1/\sqrt{2})/3 \qquad \text{(A13)}
$$

The result (A13) implies that when (A2) holds the interface is always rough and indeed the prefactor does not depend on g.

In the case $p = 0$ we see from (A2) that $g = 2$ and we are clearly in the moving phase of our original growth model. When $g = 1$ it is easy to check that we have detailed balance so that the interface is in equilibrium and again we expect it to be rough. Equation (A13) verifies that in the case of non-zero p (and when (A2) holds) the interface is rough whether it be moving upwards ($g > 1$), downwards ($g < 1$) or not at all ($g = 1$).

[1] *Random Fluctuations and Pattern Growth*, ed. by H.E. Stanley and N. Ostrowsky (Kluwer Scientific, Boston, 1988); P. Meakin, in *Phase Transitions and Critical Phenomena*, ed. by C. Domb and J. L. Lebowitz (Academic, New-York, 1988), vol. 12, p. 355.

[2] M. Kardar, G. Parisi, Y. C. Zhang, Phys. Rev. Lett. **56**, 889 (1986)

[3] J. Krug and H. Spohn, in *Solids Far From Equilibrium*, (ed. by C. Godrèche) (Cambridge University Press, New York 1991).

[4] T. Halpin-Healy and Y. C. Zhang, Physics Reports **254**, 215 (1995).

[5] B. Schmittmann and R.K.P Zia, in *Phase Transitions and Critical Phenomena*, ed. by C. Domb and J.L. Lebowitz (Academic, London, 1995), vol. 17.

[6] D. Richardson, Proc. Camb. Phil. Soc., **74**, 515 (1973).

[7] N. Goldenfeld, J. Phys. **A 17**, 2807 (1984).

[8] J. M. Kim, J. M. Kosterlitz, Phys. Rev. Lett. **62**, 2289 (1989).

[9] J. Kertész and D. E. Wolf, Phys. Rev. Lett. **62**, 2571 (1989).

[10] J. Krug, J. Kertész and D. E. Wolf, Europhys. Lett. **12**, 113 (1990).

[11] Z. Rácz, M. Siegert, D. Liu and M. Plischke, Phys. Rev. A **43**, 5275 (1991).

[12] L-H Tang, B. M. Forrest and D. E. Wolf, Phys. Rev. A **45**, 7192 (1992).

[13] D. J. Gates and M. Westcott, J. Stat. Phys **77**, 199 (1994); Proc. R. Soc. Lond. A **416**, 443 (1988).

[14] J. Neergaard and M. den Nijs, J. Phys. A **30**, 1935 (1997).

[15] C. Lehner, N. Rajewsky, D. E. Wolf and J. Kertész, Physica A **164**, 81 (1990).

[16] A. Toom, J. Stat. Phys. **74**, 91 (1994); J. Stat. Phys. **74**, 111 (1994).

[17] U. Alon, M.R. Evans, H. Hinrichsen and D. Mukamel, Phys. Rev. Lett. **76**, 2746 (1996).

[18] W. Kinzel, in *Percolation Structures and Processes*, ed. by G. Deutscher, R. Zallen, J. Adler, Annals of the Israel Physical Society, Vol **5**. (Hilger, Bristol, 1983).

[19] R. Durrett, *Lecture Notes on Particle Systems and Percolation* (Wadsworth, Pacific Grove, California 1988).

[20] J. L. Cardy and R. L. Sugar, J. Phys. A **13**, L423 (1980).

[21] E. Domany and W. Kinzel, Phys. Rev. Lett. **53**, 311 (1984).

[22] Here we consider a system to be out of equilibrium if its dynamics does not obey detailed balance.

[23] M. R. Evans, D. P. Foster, C. Godrèche, and D. Mukamel, Phys. Rev. Lett. **74**, 208 (1995); J. Stat. Phys. **80**, 69 (1995).
[24] C. Godrèche, J. M. Luck, M. R. Evans, D. Mukamel, S. Sandow, and E. R. Speer, J. Phys. **A 28**, 6039 (1995).
[25] R. Dickman, J. Stat. Phys. **55**, 997 (1989).
[26] I. Jensen and R. Dickman, J. Stat. Phys. **71**, 89 (1993).
[27] W. Kinzel, Z. Phys. B **58**, 229 (1985).
[28] I. Jensen and A. J. Guttmann, J. Phys. **A 28**, 4813 (1995); I. Jensen, Phys. Rev. Lett. **77**, 4988 (1996).
[29] J. M. Kosterlitz and D. J. Thouless, J. Phys. C 6, 1181 (1973); *ibid* C 7, 1046 (1974).
[30] H. K. Janssen, Z. Phys. **B 42**, 151 (1981).
[31] M. Doi, J. Phys. A **9**, 1479 (1976); P. Grassberger and P. Scheunert, Fortschr. Phys. **51**, 1479 (1980); L. Peliti, J. Phys. (Paris) **46**, 1469 (1984); B. P. Lee, J. Phys. **A 27**, 2633 (1994).
[32] U. C. Täuber, M. J. Howard, and H. Hinrichsen, (unpublished).
[33] P. Grassberger, (unpublished).